Molecular Neurobiology (2019) 56:4539–4548
https://doi.org/10.1007/s12035-018-1398-9

Blockade of Rapid Influx of Extracellular Zn^{2+} into Nigral Dopaminergic Neurons Overcomes Paraquat-Induced Parkinson's Disease in Rats

Haruna Tamano[1] · Hiroki Morioka[1] · Ryusuke Nishio[1] · Azusa Takeuchi[1] · Atsushi Takeda[1]

Received: 7 September 2018 / Accepted: 14 October 2018 / Published online: 19 October 2018

Abstract

The herbicide paraquat (PQ) has been reported to enhance the risk of developing Parkinson's disease (PD) from epidemiological studies. PQ-induced reactive oxygen species (ROS) are linked with a selective loss of nigrostriatal dopaminergic neurons. Here, we first report a unique mechanism of nigrostriatal dopaminergic degeneration, in which rapid intracellular Zn^{2+} dysregulation via PQ-induced ROS production causes PD in rats. When the substantia nigra pars compacta (SNpc) of rats was perfused with PQ, extracellular concentrations of glutamate and Zn^{2+} were increased and decreased, respectively, in the SNpc. These changes were ameliorated by co-perfusion with Trolox, an antioxidative agent. In in vitro slice experiments, PQ rapidly increased extracellular Zn^{2+} influx via AMPA receptor activation. Both loss of nigrostriatal dopaminergic neurons and increase in turning behavior in response to apomorphine were markedly reduced by coinjection of PQ and intracellular Zn^{2+} chelator, i.e., ZnAF-2DA into the SNpc. Furthermore, loss of nigrostriatal dopaminergic neurons induced with a low dose of PQ, which did not induce any behavioral abnormality, was completely blocked by coinjection of ZnAF-2DA. The present study indicates that rapid influx of extracellular Zn^{2+} into dopaminergic neurons via AMPA receptor activation, which is initially induced by PQ-mediated ROS production in the SNpc, induces nigrostriatal dopaminergic degeneration, resulting in PQ-induced PD in rats. Intracellular Zn^{2+} dysregulation in dopaminergic neurons is the cause of PQ-induced pathogenesis in the SNpc, and the block of intracellular Zn^{2+} toxicity leads to defending PQ-induced pathogenesis.

Keywords Zn^{2+} · Dopaminergic neuron · Substantia nigra · Striatum · Paraquat · Herbicide · Parkinson's disease

Introduction

Parkinson's disease (PD) is the second most common age-related neurodegenerative disorder [1]. The majority (~90%) of PD affecting more than 1% of the population over 60 years of age is sporadic, and aging is the major risk factor [2]. PD is characterized by a selective loss of dopaminergic neurons in the substantia nigra pars compacta (SNpc) of the brain. However, the exact cause of the neuronal loss remains unclear [3]. The environment plays a critical role in the etiology of sporadic PD. Human epidemiological studies have reported that exposure to herbicides, pesticides, and heavy metals increases the risk of PD [4, 5].

Paraquat (1,1′-dimethyl-4,4′-bipyridinium dichloride, PQ) is a herbicide widely used and is a key risk factor of PD. Epidemiologic studies have indicated the association between chronic exposure to PQ and increased risk for developing PD [6, 7]. The molecular mechanisms of PQ toxicity in nigrostriatal dopaminergic neurons are still well not understood [8, 9]. This molecule exists naturally as a divalent cation (PQ^{2+}) and undergoes redox cycling with cellular diaphorases such as NADPH oxidase and nitric oxide synthase to yield PQ^{+}, a monovalent cation that passes through dopamine transporters. Superoxide and reactive oxygen species (ROS) are produced from the redox cycling in both extracellular and intracellular compartments, followed by oxidative stress-related neurotoxicity [10, 11].

On the other hand, PQ induces the increase in extracellular glutamate to initiate excitotoxicity of neuronal nitric oxide synthase in the striatum of freely moving rats, resulting in Ca^{2+} influx via N-methyl-D-aspartate (NMDA) receptor activation. The influx of Ca^{2+} into cells stimulates nitric oxide synthase, and released NO induces long-lasting dopamine overflow in the striatum [12]. The involvement of glutamate excitotoxicity

✉ Atsushi Takeda
takedaa@u-shizuoka-ken.ac.jp

[1] Department of Neurophysiology, School of Pharmaceutical Sciences, University of Shizuoka, 52-1 Yada, Suruga-ku, Shizuoka 422-8526, Japan

in PQ-induced pathophysiology leads to an idea for the pathogenesis. Ca^{2+} influx through NMDA receptors has been believed to be a trigger for neuronal death [13, 14], while it has been recognized that the death signaling associated with neurological disorders is mediated by not only Ca^{2+} but also Zn^{2+} [15–19]. The rapid influx of extracellular Zn^{2+}, which is dynamically linked with Zn^{2+} release from zincergic neurons, a subclass of glutamatergic neurons, causes the selective and delayed degeneration of hippocampal CA1 pyramidal neurons after transient global ischemia [20–22].

In the SNpc, glutamatergic neurons are non-zincergic and do not contain zinc in the presynaptic vesicles [23]. The basal (static) concentration of extracellular Zn^{2+} is very low and estimated to be approximately 10 nM in the hippocampus [24, 25]. Because it is estimated that extracellular Zn^{2+} concentration is not appreciably modified by glutamatergic excitation in the SNpc unlike in the CA1, no attention has been paid to synaptic Zn^{2+} neurotoxicity in the SNpc. Here, we report a unique mechanism of nigrostriatal dopaminergic degeneration, in which rapid intracellular Zn^{2+} dysregulation via PQ-induced ROS production causes PD in rats.

Materials and Methods

Animals and Chemicals

Male Wistar rats (10–15 weeks of age) were purchased from Japan SLC (Hamamatsu, Japan). The rats were housed under standard laboratory conditions (23 ± 1 °C, 55 ± 5% humidity) and had access to tap water and food ad libitum. All experiments were performed in accordance with the Guidelines for the Care and Use of Laboratory Animals of the University of Shizuoka that refer to the American Association for Laboratory Animals Science and the guidelines laid down by the NIH (NIH Guide for the Care and Use of Laboratory Animals) in the USA. The ethics committee of the University of Shizuoka has approved all experimental protocols (approval number, 136043).

ZnAF-2DA, a membrane-permeable Zn^{2+} fluorescence probe, was kindly supplied by Sekisui Medical Co., LTD (Hachimantai, Japan). ZnAF-2DA is taken up into the cells through the cell membrane and is hydrolyzed by esterase in the cytosol to yield ZnAF-2, which cannot permeate the cell

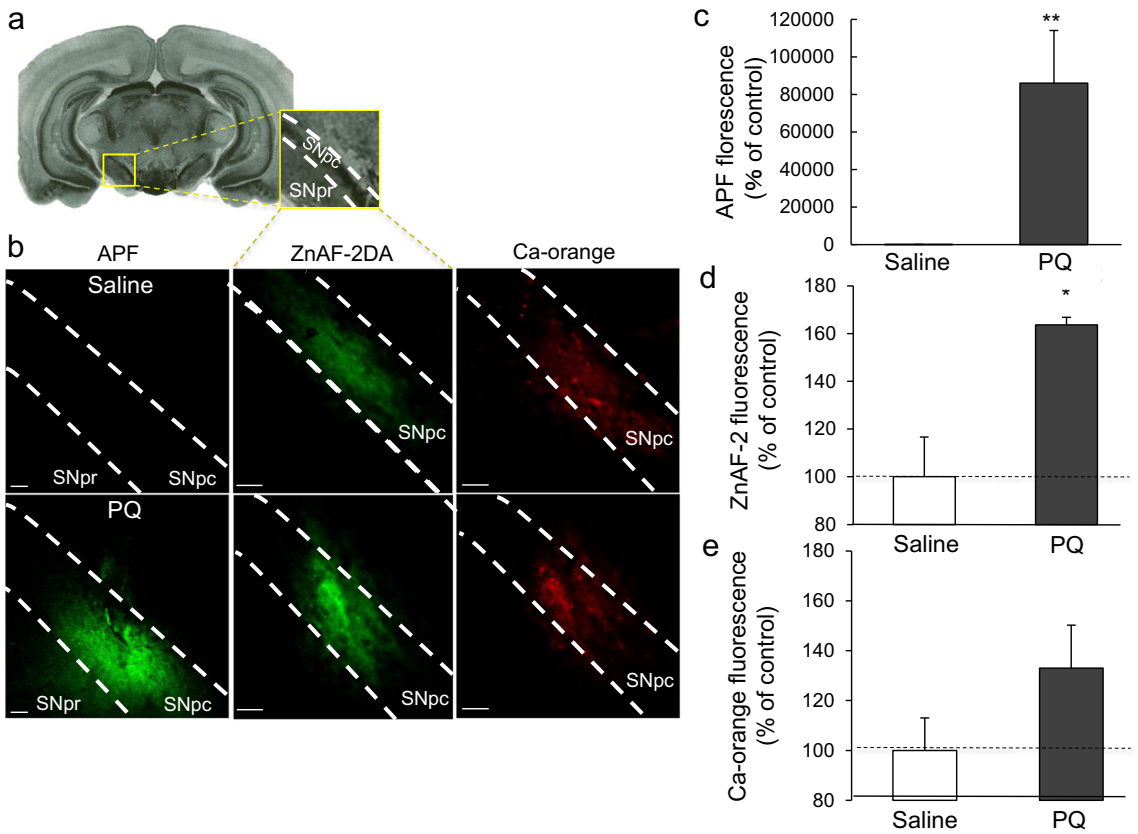

Fig. 1 In vivo imaging of ROS, intracellular Zn^{2+}, and intracellular Ca^{2+} after exposure to PQ. A, The substantia nigra and magnified substantia nigra that are surrounded with the yellow line are shown in the coronal brain image. B, Saline (control) or PQ (12 mM) in saline containing APF (10 μM) or ZnAF-2DA (100 μM) + calcium orange AM (50 μM) was bilaterally injected into the SNpc. The fluorescence of APF, ZnAF-2, and calcium orange was measured in the SNpc, which is surrounded by the white dotted line. Each bar and line represents the ratio of APF (C, $n = 5$), ZnAF-2 (D, $n = 4$), and Ca-orange (E, $n = 5$) fluorescence intensity to each control fluorescence intensity (APF, $n = 5$; ZnAF-2DA, $n = 5$; Ca-orange, $n = 7$), which was expressed as 100%. One asterisk, $p < 0.01$, two asterisks, $p < 0.005$, vs. control (t test)

membrane [26, 27]. ZnAF-2 is selectively bound to Zn^{2+}, but not bound to other divalent cations such as Ca^{2+}, Mg^{2+}, and Cu^{2+} [26]. Calcium orange AM, a membrane-permeable Ca^{2+} indicator, was purchased from Molecular Probes, Inc. (Eugene, OR). Aminophenyl fluorescence (APF), a ROS fluorescence probe, e.g., hydroxyl radical and peroxynitrite, was purchased from Sekisui Medical Co., LTD.

In Vivo Imaging of ROS and Intracellular Zn^{2+} and Ca^{2+}

The rats were anesthetized with chloral hydrate (400 mg/kg) and individually placed in a stereotaxic apparatus. The skull was exposed, a burr hole was drilled, and injection cannulae (internal diameter, 0.15 mm; outer diameter, 0.35 mm) were carefully and slowly inserted into the right and left SNpc (5.3 mm posterior to the bregma, 2.0 mm lateral, 7.0 mm inferior to the dura) to avoid cellular damages. Thirty minutes after the surgical operation, saline or 12 mM PQ in saline, which contains APF (10 μM) or ZnAF-2DA (100 μM) + calcium orange AM (50 μM), was bilaterally injected into the SNpc via cannulae at the rate of 0.2 μl/min for 5 min. Five minutes after injection, the injection cannulae were slowly pulled out of the brain in about 3 min and the rats were decapitated. The brain was quickly removed and immersed in ice-cold choline-artificial cerebrospinal fluid (ACSF) containing 124 mM choline chloride, 2.5 mM KCl, 2.5 mM $MgCl_2$, 1.25 mM NaH_2PO_4, 0.5 mM $CaCl_2$, 26 mM $NaHCO_3$, and 10 mM glucose (pH 7.3) to avoid neuronal excitation. Coronal brain slices (400 μm) were prepared using a vibratome ZERO-1 (Dosaka, Kyoto, Japan) in an ice-cold choline-ACSF and maintained in an ice-cold choline-ACSF for 30 min. The brain slices were transferred to a recording chamber filled with ACSF [119 mM NaCl, 2.5 mM KCl, 1.3 mM $MgSO_4$, 1.0 mM NaH_2PO_4, 2.5 mM $CaCl_2$, 26.2 mM $NaHCO_3$, and 11 mM D-glucose (pH 7.3)]. The fluorescence of APF (laser, 490 nm; emission, 500–550 nm), ZnAF-2 (laser, 488.4 nm; emission, 500–550 nm), and calcium orange (laser, 561.4 nm; emission, 570–620 nm) was measured with a confocal laser-scanning microscopic system (Nikon A1 confocal microscopes, Nikon Corp.) The region of interest was set in the SNpc.

In Vivo Microdialysis

A microdialysis probe (1-mm membrane, Eicom, Kyoto) was inserted into the right SNpc (5.3 mm posterior to the bregma, 2.0 mm lateral, 7.8 mm inferior to the dura) of the rats as described above. The SNpc was preperfused with ACSF (127 mM NaCl, 2.5 mM KCl, 1.3 mM $CaCl_2$, 0.9 mM $MgCl_2$, 1.2 mM Na_2HPO_4, 21 mM $NaHCO_3$, and 3.4 mM D-glucose, pH 7.3) at 2.0 μl/min for 120 min to stabilize the region; perfused with ACSF for 60 min in the same manner to determine the basal concentration of extracellular Zn^{2+}, glutamate, and γ-aminobutyric acid (GABA); and then perfused with 12 mM PQ in ACSF or 12 mM PQ + 1 mM Trolox (6-hydroxy-2,5,7,8-tetramethylchroman-2-carboxylic acid), an antioxidative agent in ACSF for 60 min.

The perfusate was collected for 15 min, and the basal levels and the levels during perfusion with PQ were averaged. ZnAF-2 (1 μM, 50 μl) was added to the aliquot of the perfusate (10 μl) for measuring extracellular Zn^{2+} levels. The fluorescence of ZnAF-2 (Ex/Em; 485/535 nm) was measured using a plate reader ARVO sx (Perkin Elmer, USA). The

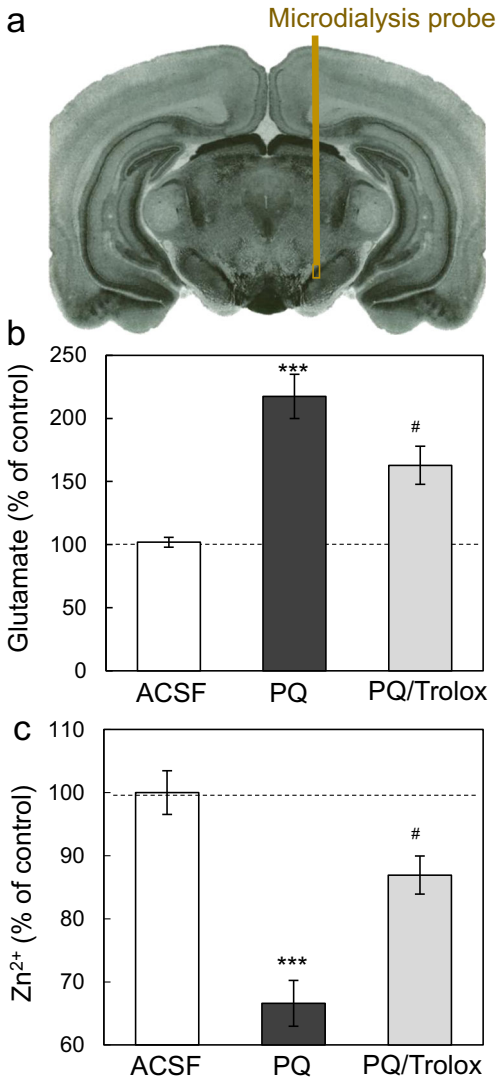

Fig. 2 PQ modifies extracellular concentrations of glutamate and Zn^{2+} in the SNpc in vivo. **a** The SNpc was perfused with 12 mM PQ in ACSF or 12 mM PQ + 1 mM Trolox in ACSF as shown in the coronal image of the rat brain. Each bar and line represents the ratio of glutamate concentration in the perfusate with PQ ($n = 5$) or PQ + Trolox ($n = 5$) (**b**) and ZnAF-2 fluorescence intensity in the perfusate with PQ ($n = 4$) or PQ + Trolox ($n = 4$) (**c**) to the basal glutamate concentration ($n = 10$) and ZnAF-2 fluorescence intensity ($n = 8$) in the perfusate, respectively, which was perfused with ACSF and expressed as 100%. Three asterisks, $p < 0.001$, vs. the basal level (ACSF); one number sign, $p < 0.01$, vs. PQ group (Tukey's test)

perfusate samples (15 μl) were also analyzed for glutamate and GABA contents by high-performance liquid chromatography (HPLC) [column, CAPCELL PAK C18 UG120A (1 mm × 150 mm) (Shiseido Co Ltd., Tokyo, Japan); mobile phase, 0.1 M potassium dihydrogen phosphate, 0.1 M disodium hydrogen phosphate, 10% acetonitrile, 0.5 mM EDTA-2Na, 3% tetrahydrofuran, pH 6.0] using the pre-column derivatization technique with o-phthaldialdehyde and a fluorescence detector (NANOSPACE SI-2, Shiseido Co Ltd).

In Vitro Dynamics of Intracellular Zn^{2+}

The brain was quickly removed from the rats under anesthesia with chloral hydrate and immersed in ice-cold choline-ACSF. Coronal brain slices (400 μm) were prepared and maintained in ice-cold choline-ACSF for 15 min. To assess intracellular levels of Zn^{2+}, brain slices were placed for 30 min in 10 μM ZnAF-2DA in ACSF; rinsed in choline-ACSF for 15 min; placed in a chamber filled with 12 mM PQ, 12 mM PQ + 10 mM CaEDTA, a membrane-impermeable Zn^{2+} chelator, or 12 mM PQ + 10 μM 6-cyano-7-nitroquinoxaline-2,3-dione (CNQX), an α-amino-3-hydroxy-5-methyl-4-isoxazolepropionate (AMPA) receptor antagonist, in ACSF containing 10 nM $ZnCl_2$ for 10 min; rinsed in choline-ACSF for 15 min; and transferred to a recording chamber filled with ACSF. The fluorescence of ZnAF-2 was measured in the same manner.

In another experiment to assess the effect of a low dose of PQ, brain slices were placed for 30 min in 10 μM ZnAF-2DA in ACSF, rinsed in choline-ACSF for 15 min, and placed in a chamber filled with 40 μM PQ, 40 μM PQ + 10 mM CaEDTA, or 40 μM PQ + 1 mM Trolox in ACSF containing 10 nM $ZnCl_2$ for 10 min. The fluorescence of ZnAF-2 was measured in the same manner.

Behavioral Studies

As described in the section "In Vivo Imaging of ROS and Intracellular Zn^{2+} and Ca^{2+}," an injection cannula was inserted into the right SNpc and 12 mM PQ or 12 mM PQ + 200 μM ZnAF-2DA in saline was unilaterally injected into the SNpc via the cannula at the rate of 0.2 μl/min for 5 min. Ten minutes after injection, the injection cannula was slowly pulled out of the brain in about 3 min. One and two weeks later, the rats were subcutaneously injected with apomorphine (0.5 mg/kg) and turning behavior in response to apomorphine was measured for 30 min after the start of the turning behavior. In another experiment, an injection cannula was inserted into the right SNpc and 40 μM PQ or 40 μM PQ + 200 μM ZnAF-2DA in saline was unilaterally injected into the SNpc via the cannula at the rate of 0.2 μl/min for 5 min. The rats were treated in the same manner.

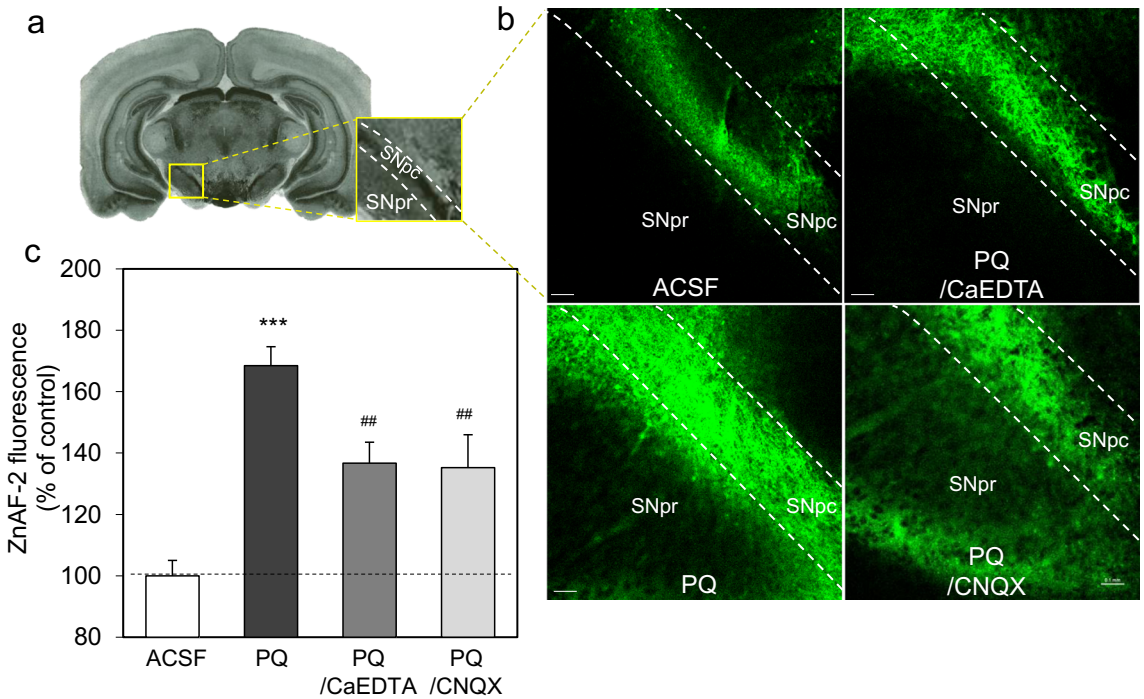

Fig. 3 PQ increases intracellular Zn^{2+} concentration in the SNpc in vitro. A, the substantia nigra and magnified substantia nigra that are surrounded with the yellow line are shown in the coronal brain image. B, brain slices loaded with ZnAF-2DA were immersed in ACSF (control, $n = 10$), 12 mM PQ in ACSF ($n = 11$), 12 mM PQ + 10 mM CaEDTA in ACSF ($n = 8$), or 12 mM PQ + 10 μM CNQX in ACSF ($n = 6$) for 10 min. Intracellular ZnAF-2 fluorescence was imaged in the SNpc. C, each bar and line represents the ratio of ZnAF-2 fluorescence intensity to the control ZnAF-2 fluorescence intensity, which was expressed as 100%. Three asterisks, $p < 0.001$, vs. control (ACSF); two number signs, $p < 0.005$, vs. PQ group (Tukey's test)

Tyrosine Hydroxylase Immunostaining

The rats were anesthetized and perfused with ice-cold 4% paraformaldehyde in PBS after the behavioral studies were finished, followed by removal of the brain and overnight fixation in 4% paraformaldehyde in PBS at 4 °C. The fixed brains were cryopreserved in 30% sucrose in PBS for 2 days and frozen in Tissue-Tek Optimal Cutting Temperature embedding medium. Coronal brain slices (30 μm) were prepared at − 20 °C in a cryostat, picked up on slides, and adhered at room temperature for 30 min. For immunostaining, the slides were incubated in blocking solution (3% BSA, 0.1% Triton X-100 in PBS) for 1 h and rinsed with PBS for 5 min followed by overnight incubation with anti-tyrosine hydroxylase antibody (Abcam) at 4 °C. The slides were rinsed with PBS for 5 min and incubated in blocking buffer containing Alexa Fluor 633 goat anti-rabbit secondary antibody (ThermoFisher) for 3 h at room temperature. Following six rinses in PBS for 5 min, the slides were mounted with Prolong Gold antifade reagent and placed for 24 h at 4 °C. Alexa Fluor 633 fluorescence was measured in the SNpc and the striatum using a confocal laser-scanning microscopic system.

Data Analysis

For statistical analysis, Student's *t* test was used for comparison of the means of paired or unpaired data. For multiple comparisons, differences between treatments were assessed by one-way ANOVA followed by post hoc testing using Tukey's test (the statistical software GraphPad Prism 5). A value of $p < 0.05$ was considered significant. Data were expressed as means ± standard error. The results of statistical analysis are described in each figure legend.

Results

PQ-Induced ROS Production Causes Intracellular Zn^{2+} Dysregulation

To assess synaptic Zn^{2+} dynamics under PQ-induced ROS production in vivo, PQ was locally coinjected with APF into the SNpc. Eight minutes later, APF fluorescence was markedly increased in the SNpc, indicating that intracellular ROS is rapidly produced with PQ in the SNpc (Fig. 1A, B). When intracellular Zn^{2+} dynamics was compared with intracellular Ca^{2+} dynamics in the same manner after injection of PQ into the SNpc, intracellular Zn^{2+} was significantly increased in the SNpc, while intracellular Ca^{2+} was not significantly increased (Fig. 1B, D, E).

To check glutamate neurotransmission under PQ-induced ROS production in vivo, the extracellular glutamate level was determined by in vivo SNpc perfusion with PQ. Extracellular glutamate concentration was increased in the SNpc (Fig. 2b), while extracellular GABA concentration was not influenced in the SNpc (basal concentrations of glutamate and GABA in the perfusate, 2.37 ± 0.34 and 0.19 ± 0.07 μM, respectively). On the other hand, the extracellular Zn^{2+} level was decreased in the SNpc under the SNpc perfusion with PQ (Fig. 2c). It is estimated that a PQ-induced increase in extracellular glutamate induces the influx of extracellular Zn^{2+} in the SNpc, resulting in the decrease in the extracellular Zn^{2+} level. Interestingly, the changes in extracellular levels of glutamate and Zn^{2+} were ameliorated under co-perfusion with Trolox, suggesting that PQ-induced ROS production increases Zn^{2+} influx via glutamate receptor activation in the SNpc.

Intracellular Zn^{2+} dynamics was also assessed by changes in intracellular ZnAF-2 fluorescence in brain slices after exposure to PQ, which were bathed in ACSF containing 10 nM Zn^{2+}, an estimated concentration of brain extracellular Zn^{2+} [24, 25]. The basal level of intracellular Zn^{2+} in the substantia nigra pars reticulata (SNpr) was 78 ± 17.8% when the basal level of intracellular Zn^{2+} in the SNpc was expressed as 100 ± 6.2% (ACSF image in Fig. 3B). Intracellular Zn^{2+} was rapidly increased in the SNpc after a 10-min incubation with PQ, and this increase was suppressed in the presence of CaEDTA, an

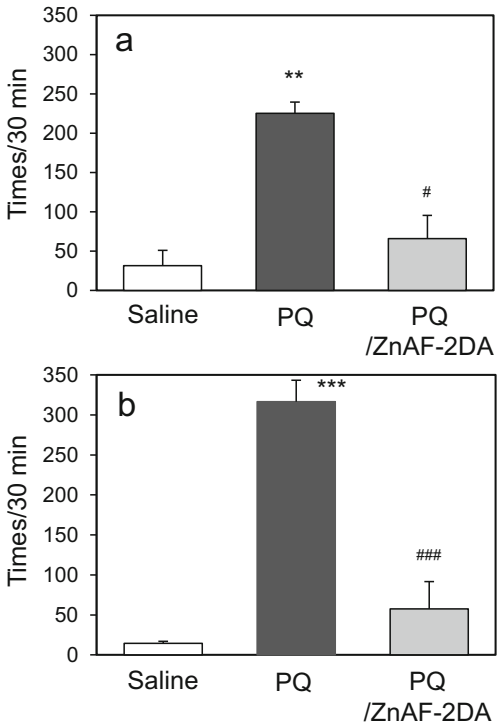

Fig. 4 Turning behavior in response to apomorphine after injection of PQ into the SNpc. Vehicle (control, $n = 5$), 12 mM PQ ($n = 5$), or 12 mM PQ + 200 μM ZnAF-2DA ($n = 7$) in saline was unilaterally injected into the SNpc. One (**a**) and two (**b**) weeks later, the rats were subcutaneously injected with apomorphine (0.5 mg/kg) and turning behavior (the number of times) in response to apomorphine was measured for 30 min after the start of the turning behavior. Two asterisks, $p < 0.005$, three asterisks, $p < 0.001$, vs. control (saline); one number sign, $p < 0.01$, three number signs, $p < 0.001$, vs. PQ group (Tukey's test)

extracellular Zn^{2+} chelator, and CNQX, an AMPA receptor antagonist, suggesting that PQ rapidly increases extracellular Zn^{2+} influx via AMPA receptor activation (Fig. 3B, C).

Intracellular Zn^{2+} Chelator Ameliorates PQ-Induced Movement Disorder and Neurodegeneration

Turning behavior in response to apomorphine, an index of movement disorder in PQ-induced PD in rats, was markedly ameliorated 1 and 2 weeks after coinjection of ZnAF-2DA with PQ (Fig. 4). Coinjection of ZnAF-2DA reduced PQ-induced turning behavior to the control level.

PQ-induced loss of nigrostriatal dopaminergic neurons was determined by tyrosine hydroxylase (TH) immunostaining after the behavioral test was finished. TH immunostaining was not performed in the SNpc because of severe tissue damage in the ipsilateral SNpc. Staining intensity was drastically reduced in the ipsilateral striatum (Fig. 5). However, the reduction was also markedly ameliorated by coinjection of ZnAF-2DA.

Intracellular Zn^{2+} Dysregulation Causes PQ Damage Without Movement Disorder

We found a dose that is one 300th of the present PQ dose. This dose did not show any changes in turning behavior, compared to the control injected with vehicle. PQ-induced loss of nigrostriatal dopaminergic neurons was determined by TH immunostaining in the same manner after the behavioral test was finished. Staining intensity was reduced to approximately 50% in the ipsilateral SNpc after injection of PQ into the SNpc (Fig. 6a, b). This reduction was almost completely blocked by coinjection of ZnAF-2DA. On the other hand, staining intensity was not reduced in the ipsilateral striatum after injection of PQ into the SNpc (Fig. 6a, c). Staining intensity was not also reduced in the ipsilateral striatum after coinjection of ZnAF-2DA.

Intracellular Zn^{2+} dynamics was assessed by changes in intracellular ZnAF-2 fluorescence in brain slices bathed in the low dose of PQ. Intracellular Zn^{2+} was rapidly increased in the SNpc after a 10-min incubation with PQ (Fig. 7) as well as the case of the high dose (Fig. 3), and this increase was reduced to almost the control level in the presence of CaEDTA and Trolox, suggesting that the rapid influx of extracellular Zn^{2+} is due to PQ-induced ROS production.

Discussion

After chronic exposure to Zn, Zn accumulates in the nigrostriatal tissues and induces oxidative stress via the activation of NADPH oxidase and depletion of GSH, which in

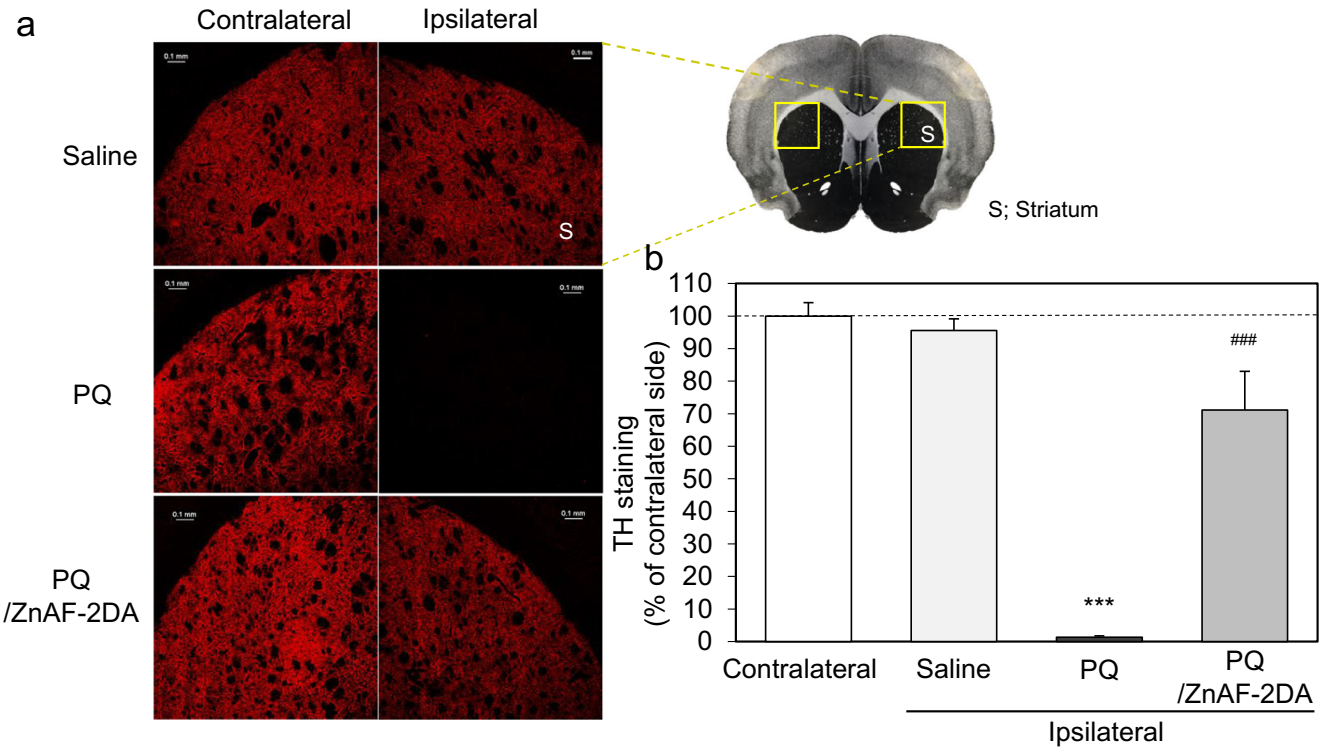

Fig. 5 Neuronal loss in the striatum after injection of PQ into the SNpc. A, brain slices were prepared from the rats after the behavioral test was finished in Fig. 4, and TH immunostaining with Alexa Fluor 633 fluorescence was performed in the striatum (S) that was surrounded by the yellow line in the coronal brain image (right). B, each bar and line represents the ratio of Alexa Fluor 633 fluorescence intensity to Alexa Fluor 633 fluorescence intensity in the control contralateral striatum, which was expressed as 100%. Three asterisks, $p < 0.001$, vs. control contralateral ($n = 8$) and ipsilateral saline ($n = 8$); three number signs, $p < 0.001$, vs. PQ group ($n = 6$) (Tukey's test). PQ/ZnAF-2DA, $n = 6$

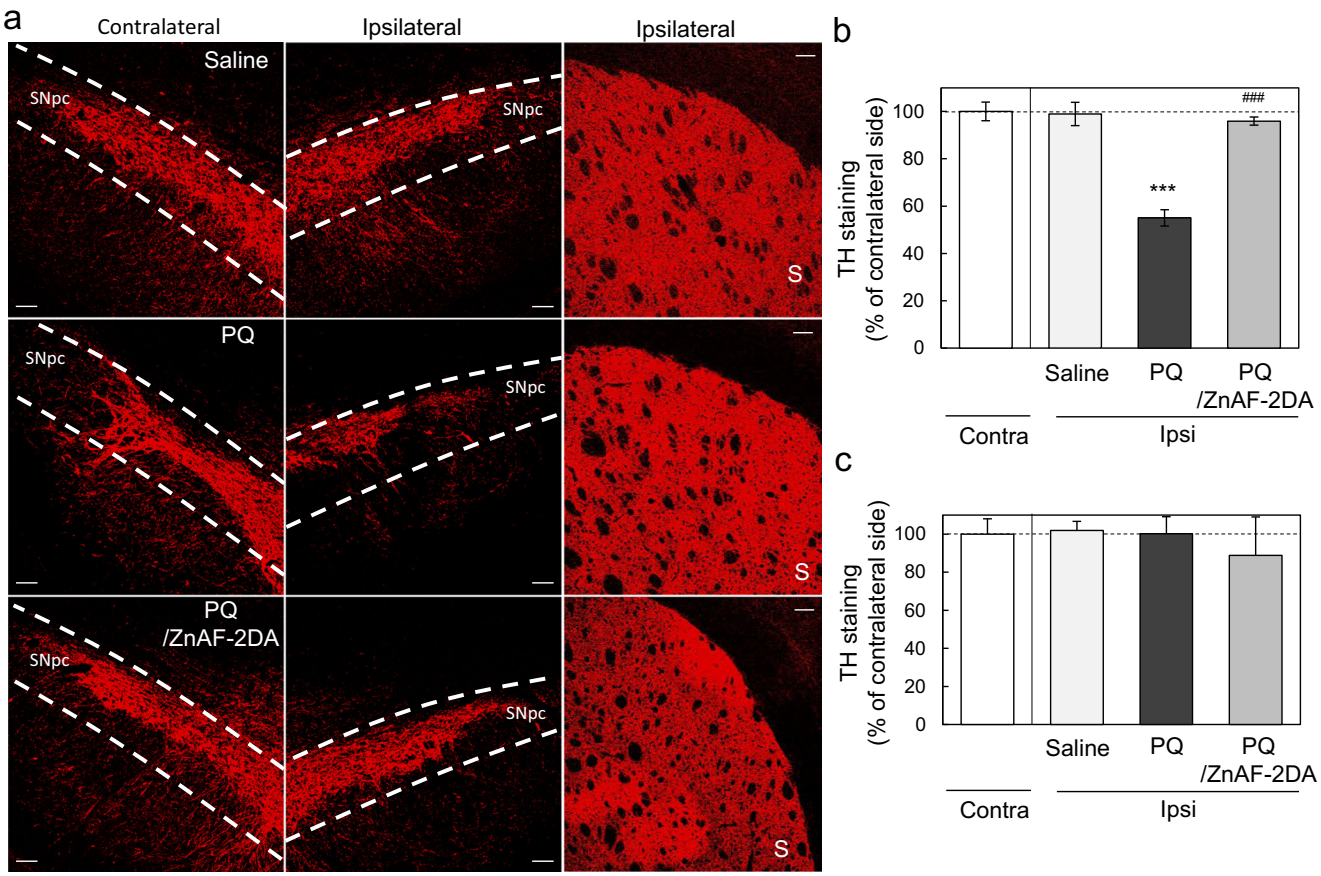

Fig. 6 Neuronal loss in the SNpc and striatum after injection of 40 μM PQ into the SNpc. **a** Brain slices were prepared from the rats in the same manner as Fig. 5 after the behavioral test was finished and TH immunostaining with Alexa Fluor 633 fluorescence was performed in the SNpc and the ipsilateral striatum. Each bar and line represents the ratio of Alexa Fluor 633 fluorescence intensity to Alexa Fluor 633 fluorescence intensity in the control contralateral SNpc (**b**) and striatum (**c**), which was expressed as 100%. Three asterisks, $p < 0.001$, vs. control contralateral and ipsilateral saline; three number signs, $p < 0.001$, vs. PQ group (Tukey's test). In the SNpc: contralateral saline, $n = 16$; ipsilateral saline, $n = 4$; ipsilateral PQ, $n = 8$; ipsilateral PQ/ZnAF-2DA, $n = 4$; in the striatum: contralateral saline, $n = 8$; ipsilateral saline, $n = 8$; ipsilateral PQ, $n = 8$; ipsilateral PQ/ZnAF-2DA, $n = 4$

turn activates the apoptotic machinery leading to dopaminergic neurodegeneration [28]. Effect of co-exposure to Zn and PQ indicates some different mechanisms between Zn and PQ leading dopaminergic neurodegeneration [29]. On the other hand, the evidence that glutamate excitotoxicity may be involved in progressive degeneration of dopaminergic neurons in PD implies involvement of free Zn^{2+} toxicity in PD pathophysiology [30, 31]. Nonetheless, there has been no report on the involvement of synaptic Zn^{2+} dynamics in nigral dopaminergic degeneration because of unappreciated extracellular Zn^{2+} concentration in the SNpc. In the present study, we postulated that nigral dopaminergic neurons are sensitive to intracellular Zn^{2+} dysregulation because intracellular Zn^{2+} concentration is estimated to be considerably low (~ 100 pM) in nigral dopaminergic neurons, compared with the basal concentration of intracellular Ca^{2+} (~ 100 nM) [32, 33]. We tested a unique mechanism, in which PQ-induced ROS production rapidly causes intracellular Zn^{2+} dysregulation, resulting in nigral dopaminergic degeneration in rats.

It is unknown whether in vivo PQ-induced ROS production modifies intracellular Zn^{2+} dynamics via glutamate neurotransmission in the SNpc. When PQ was locally coinjected with ZnAF-2DA into the SNpc, ROS production and the intracellular Zn^{2+} level, unlike the intracellular Ca^{2+} level, were concurrently increased in the SNpc, suggesting that PQ-induced ROS production rapidly induces intracellular Zn^{2+} dysregulation. It is possible that this dysregulation is due to extracellular glutamate accumulation via PQ-induced ROS production. We tested the possibility by using in vivo microdialysis. Extracellular glutamate concentration was increased in the SNpc under perfusion with PQ, while extracellular Zn^{2+} concentration was decreased in the SNpc. The opposite changes in extracellular levels of glutamate and Zn^{2+} were ameliorated under co-perfusion with Trolox. These results suggest that PQ-induced ROS production rapidly increases Zn^{2+} influx via glutamate receptor activation in the SNpc. Because PQ is taken up into dopaminergic neurons through dopamine transporter as PQ^{+}, a monovalent cation, PQ-

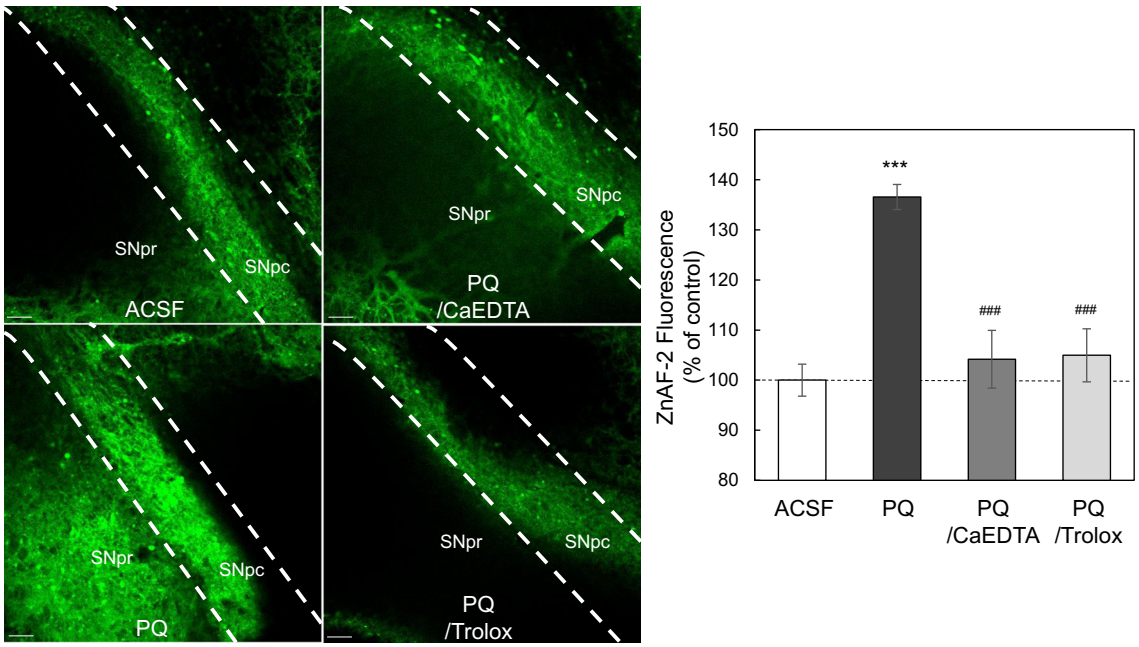

Fig. 7 PQ increases intracellular Zn^{2+} concentration in the SNpc in vitro. Brain slices loaded with ZnAF-2DA were immersed in ACSF (control, $n = 7$), 40 μM PQ in ACSF ($n = 7$), 40 μM PQ + 10 mM CaEDTA in ACSF ($n = 5$), or 40 μM PQ + 1 mM Trolox in ACSF ($n = 4$) for 10 min. Intracellular ZnAF-2 fluorescence was imaged in the SNpc (left). Each bar and line represents the ratio of ZnAF-2 fluorescence intensity to the control ZnAF-2 fluorescence intensity, which was expressed as 100% (right). Three asterisks, $p < 0.001$, vs. control (ACSF); three number signs, $p < 0.001$, vs. PQ group (Tukey's test)

induced ROS is increased in both extracellular and intracellular compartments (Fig. 8). It is estimated that PQ-induced ROS increases glutamate exocytosis via unknown mechanisms. Alternatively, it is possible that PQ-induced ROS blocks glutamate transporter activity. PQ rapidly increased intracellular Zn^{2+} in the SNpc of brain slices bathed in ACSF containing 10 nM Zn^{2+}, and this increase was blocked in the presence of CaEDTA and CNQX, suggesting that the rapid influx of extracellular Zn^{2+} occurs via AMPA receptor activation in the SNpc after exposure to PQ, followed by intracellular Zn^{2+} dysregulation. It has been reported that the rapid influx of extracellular Zn^{2+} via AMPA receptor activation into dentate granule cells, which are innervated by non-zincergic neurons, induces cognitive decline [34–36]. GluR2-

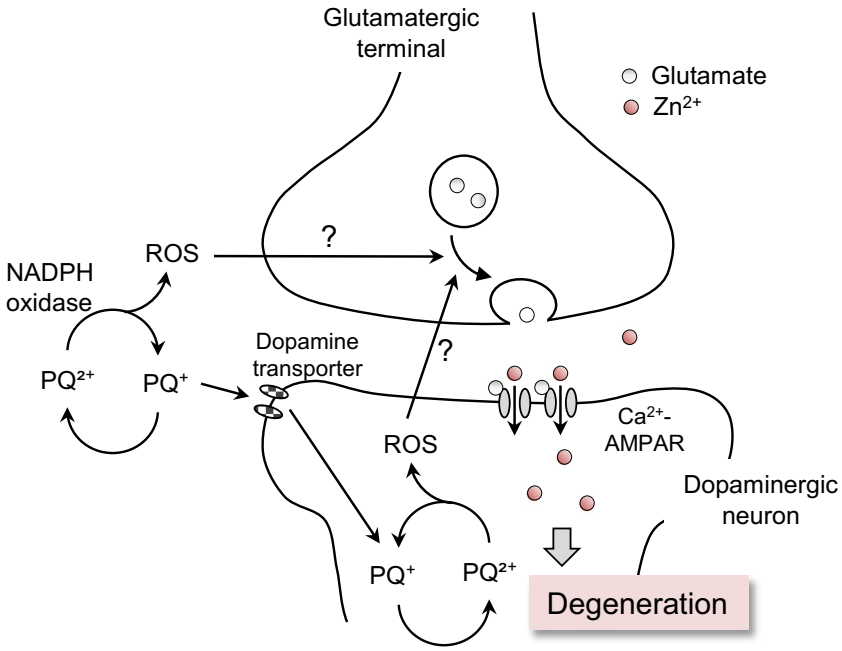

Fig. 8 Proposed mechanism of PQ-induced PD in rats. Rapid influx of extracellular Zn^{2+} into dopaminergic neurons via AMPA receptor activation in the SNpc, which is induced by PQ-mediated ROS production, causes nigrostriatal dopaminergic degeneration, resulting in PQ-induced PD in rats

lacking Ca^{2+}-permeable AMPA receptors are involved in Zn^{2+}-mediated neurodegeneration in the hippocampal CA1 [21, 37, 38]. Extracellular Zn^{2+} preferentially passes through Ca^{2+}-permeable AMPA receptors in the hippocampus. When intracellular Zn^{2+} concentration (~ 100 pM) in dentate granule cells reaches near to extracellular Zn^{2+} concentration (~10 nM), it may lead to cognitive decline. Thus, it is possible that rapid intracellular Zn^{2+} dysregulation leads to neuronal death even under non-zincergic innervation (Fig. 8).

Both PQ-induced loss of nigrostriatal dopaminergic neurons and turning behavior in response to apomorphine were markedly reduced by coinjection of intracellular Zn^{2+} chelator, i.e., ZnAF-2DA, suggesting that the block of PQ-induced rapid increase in intracellular Zn^{2+} with intracellular ZnAF-2 protects nigrostriatal dopaminergic neurons against degeneration. In 6-hydroxydopamine (6-OHDA)-induced PD in rats, ZnAF-2DA also suppresses not only increased turning behavior in response to apomorphine but also nigrostriatal dopaminergic neurodegeneration, which are due to 6-OHDA-induced extracellular Zn^{2+} influx into nigral dopaminergic neurons [39]. 6-OHDA-induced extracellular Zn^{2+} influx is completely blocked in the presence of CaEDTA and CNQX. In contrast, PQ-induced increase in intracellular Zn^{2+} was also significantly reduced in the presence of CaEDTA and CNQX, while the reduction was partial, suggesting Zn^{2+} release forms internal stores in addition to extracellular Zn^{2+} influx. PQ-mediated mitochondrial dysfunction including ROS generation promotes intracellular Zn^{2+} mobilization, which originates in the mitochondria and metallothioneins [40, 41]. Among metallothionein isoforms, metallothionein III preferentially releases Zn^{2+} under oxidative condition [42]. ROS-mediated TRPM7 (transient receptor potential cation channel subfamily M member 7) activation releases Zn^{2+} from intracellular vesicles after Zn^{2+} overload [43]. It is likely that Zn^{2+} release from metallothioneins and/or internal stores collaborates with Zn^{2+} influx for neurodegeneration. PQ-mediated ROS production leads to extracellular glutamate accumulation and rapid intracellular Zn^{2+} dysregulation in the SNpc. Iron and PQ are synergistic environmental risk factors in sporadic PD and accelerate age-related neurodegeneration [44]. Iron enhances PQ-induced dopaminergic cell death via increased oxidative stress [45].

On the other hand, it is possible that the rapid Zn^{2+} influx via PQ-mediated ROS production in the SNpc is the cause of PQ-induced dopaminergic cell death. To pursue the possibility, we used a low dose of PQ, which did not show any movement disorder. Dopaminergic neurons were reduced to approximately 50% only in the ipsilateral SNpc after injection of PQ into the SNpc, and this reduction was almost completely blocked by coinjection of ZnAF-2DA. It is estimated that blocking toxic intracellular Zn^{2+} with intracellular ZnAF-2 is effective for at longest 1 h after injection of PQ into the SNpc [46]. Furthermore, CaEDTA almost completely blocked PQ-induced rapid increase in intracellular Zn^{2+} in brain slices, which was due to PQ-induced ROS production. Therefore, rapid intracellular Zn^{2+} dysregulation via extracellular Zn^{2+} influx, which is initially induced by PQ-mediated ROS production, is critical for PQ-induced pathogenesis in the SNpc. Zn^{2+} release from metallothioneins and/or internal stores scarcely contributes to PQ-induced PD.

In conclusion, the present study indicates that rapid influx of extracellular Zn^{2+} into dopaminergic neurons via AMPA receptor activation, which is initially induced by PQ-mediated ROS production in the SNpc, induces nigrostriatal dopaminergic degeneration, resulting in PQ-induced PD in rats (Fig. 8). Intracellular Zn^{2+} dysregulation in dopaminergic neurons is the cause of PQ-induced pathogenesis in the SNpc. The block of intracellular Zn^{2+} toxicity may be an effective strategy for defending PQ-induced pathogenesis.

Compliance with Ethical Standards

All experiments were performed in accordance with the Guidelines for the Care and Use of Laboratory Animals of the University of Shizuoka that refer to the American Association for Laboratory Animals Science and the guidelines laid down by the NIH (NIH Guide for the Care and Use of Laboratory Animals) in the USA. The ethics committee of the University of Shizuoka has approved all experimental protocols (approval number, 136043).

Conflict of Interest The authors declare that they have no conflict of interest.

References

1. Olanow CW, Tatton WG (1999) Etiology and pathogenesis of Parkinson's disease. Annu Rev Neurosci 22:123–144
2. de Lau LM, Breteler MM (2006) Epidemiology of Parkinson's disease. Lancet Neurol 5:525–535
3. Zhai S, Tanimura A, Graves SM, Shen W, Surmeier DJ (2017) Striatal synapses, circuits, and Parkinson's disease. Curr Opin Neurobiol 48:9–16
4. Tanner CM, Kamel F, Ross GW, Hoppin JA, Goldman SM, Korell M, Marras C, Bhudhikanok GS et al (2011) Rotenone, paraquat, and Parkinson's disease. Environ Health Perspect 119:866–872
5. Ritz BR, Paul KC, Bronstein JM (2016) Of pesticides and men: a California story of genes and environment in Parkinson's disease. Curr Environ Health Rep 3:40–52
6. Hertzman C, Wiens M, Bowering D, Snow B, Calne D (1990) Parkinson's disease: a case-control study of occupational and environmental risk factors. Am J Ind Med 17:349–355
7. Liou HH, Tsai MC, Chen CJ, Jeng JS, Chang YC, Chen SY, Chen RC (1997) Environmental risk factors and Parkinson's disease: a case-control study in Taiwan. Neurology 48:1583–1588
8. Zhang XF, Thompson M, Xu YH (2016) Multifactorial theory applied to the neurotoxicity of paraquat and paraquat-induced mechanisms of developing Parkinson's disease. Lab Investig 96:496–507
9. Vaccari C, El Dib R, de Camargo JLV (2017) Paraquat and Parkinson's disease: a systematic review protocol according to the OHAT approach for hazard identification. Syst Rev 6:98

10. Kellendonk C, Simpson EH, Polan HJ, Malleret G, Vronskaya S, Winiger V, Moore H, Kandel ER (2006) Transient and selective overexpression of dopamine D2 receptors in the striatum causes persistent abnormalities in prefrontal cortex functioning. Neuron 49:603–615
11. Drechsel DA, Patel M (2008) Role of reactive oxygen species in the neurotoxicity of environmental agents implicated in Parkinson's disease. Free Radic Biol Med 44:1873–1886
12. Shimizu K, Matsubara K, Ohtaki K, Fujimaru S, Saito O, Shiono H (2003) Paraquat induces long-lasting dopamine overflow through the excitotoxic pathway in the striatum of freely moving rats. Brain Res 976:243–252
13. Ambrosi G, Cerri S, Blandini F (2014) A further update on the role of excitotoxicity in the pathogenesis of Parkinson's disease. J Neural Transm (Vienna) 121:849–859
14. Oster S, Radad K, Scheller D, Hesse M, Balanzew W, Reichmann H, Gille G (2014) Rotigotine protects against glutamate toxicity in primary dopaminergic cell culture. Eur J Pharmacol 724:31–42
15. Weiss JH, Sensi SL (2000) Ca2+-Zn2+ permeable AMPA or kainate receptors: possible key factors in selective neurodegeneration. Trends Neurosci 23:365–371
16. Frederickson CJ, Koh JY, Bush AI (2005) The neurobiology of zinc in health and disease. Nat Rev Neurosci 6:449–462
17. Sensi SL, Paoletti P, Bush AI, Sekler I (2009) Zinc in the physiology and pathology of the CNS. Nat Rev Neurosci 10:780–791
18. Pochwat B, Nowak G, Szewczyk B (2015) Relationship between zinc (Zn (2+)) and glutamate receptors in the processes underlying neurodegeneration. Neural Plast 2015:591563
19. Takeda A, Tamano H (2016) Insight into cognitive decline from Zn^{2+} dynamics through extracellular signaling of glutamate and glucocorticoids. Arch Biochem Biophys 611:93–99
20. Koh JY, Suh SW, Gwag BJ, He YY, Hsu CY, Choi DW (1996) The role of zinc in selective neuronal death after transient global cerebral ischemia. Science 272:1013–1016
21. Liu S, Lau L, Wei J, Zhu D, Zou S, Sun HS, Fu Y, Liu F et al (2004) Expression of Ca(2+)-permeable AMPA receptor channels primes cell death in transient forebrain ischemia. Neuron 43:43–55
22. Noh KM, Yokota H, Mashiko T, Castillo PE, Zukin RS, Bennett MV (2005) Blockade of calcium-permeable AMPA receptors protects hippocampal neurons against globalischemia-induced death. Proc Natl Acad Sci U S A 102:12230–12235
23. Frederickson CJ (1989) Neurobiology of zinc and zinc-containing neurons. Int Rev Neurobiol 31:145–238
24. Frederickson CJ, Giblin LJ, Krezel A, McAdoo DJ, Muelle RN, Zeng Y, Balaji RV, Masalha R et al (2006) Concentrations of extracellular free zinc (pZn)e in the central nervous system during simple anesthetization, ischemia and reperfusion. Exp Neurol 198:285–293
25. Tamano H, Nishio R, Shakushi Y, Sasaki M, Koike Y, Osawa M, Takeda A (2017) In vitro and in vivo physiology of low nanomolar concentrations of Zn^{2+} in artificial cerebrospinal fluid. Sci Rep 7:42897
26. Hirano T, Kikuchi K, Urano Y, Nagano T (2002) Improvement and biological applications of fluorescent probes for zinc, ZnAFs. J Am Chem Soc 124:6555–6562
27. Ueno S, Tsukamoto M, Hirano T, Kikuchi K, Yamada MK, Nishiyama N, Nagano T, Matsuki N et al (2002) Mossy fiber Zn^{2+} spillover modulates heterosynaptic *N*-methyl-*D*-aspartate receptor activity in hippocampal CA3 circuits. J Cell Biol 158:215–220
28. Kumar A, Singh BK, Ahmad I, Shukla S, Patel DK, Srivastava G, Kumar V, Pandey HP et al (2012) Involvement of NADPH oxidase and glutathione in zinc-induced dopaminergic neurodegeneration in rats: similarity with paraquat neurotoxicity. Brain Res 1438:48–64
29. Kumar A, Ahmad I, Shukla S, Singh BK, Patel DK, Pandey HP, Singh C (2010) Effect of zinc and paraquat co-exposure on neurodegeneration: modulation of oxidative stress and expression of metallothioneins, toxicant responsive and transporter genes in rats. Free Radic Res 44:950–965
30. Beal MF (1998) Excitotoxicity and nitric oxide in Parkinson's disease pathogenesis. Ann Neurol 44:S110–S114
31. Zhang L, Dawson VL, Dawson TM (2006) Role of nitric oxide in Parkinson's disease. Pharmacol Ther 109:33–41
32. Sensi SL, Canzoniero LMT, Yu SP, Ying HS, Koh JY, Kerchner GA, Choi DW (1997) Measurement of intracellular free zinc in living cortical neurons: routes of entry. J Neurosci 15:9554–9564
33. Colvin RA, Bush AI, Volitakis I, Fontaine CP, Thomas D, Kikuchi K, Holmes WR (2008) Insights into Zn2+ homeostasis in neurons from experimental and modeling studies. Am J Physiol Cell Physiol 294:C726–C742
34. Suzuki M, Fujise Y, Tsuchiya Y, Tamano H, Takeda A (2015) Excess influx of Zn^{2+} into dentate granule cells affects object recognition memory via attenuated LTP. Neurochem Int 87:60–65
35. Takeda A, Tamano H, Hisatsune M, Murakami T, Nakada H, Fujii H (2018) Maintained LTP and memory are lost by Zn^{2+} influx into dentate granule cells, but not Ca^{2+} influx. Mol Neurobiol 55:1498–1508
36. Takeda A, Koike Y, Osawa M, Tamano H (2018) Characteristic of extracellular Zn^{2+} influx in the middle-aged dentate gyrus and its involvement in attenuation of LTP. Mol Neurobiol 55:2185–2195
37. Colbourne F, Grooms SY, Zukin RS, Buchan AM, Bennett MV (2003) Hypothermia rescues hippocampal CA1 neurons and attenuates down-regulation of the AMPA receptor GluR2 subunit after forebrain ischemia. Proc Natl Acad Sci U S A 100:2906–2910
38. Weiss JH (2011) Ca permeable AMPA channels in diseases of the nervous system. Front Mol Neurosci 4:42
39. Tamano H, Nishio R, Morioka H, Takeda A (2018) Extracellular Zn^{2+} influx into nigral dopaminergic neurons plays a key role for pathogenesis of 6-hydroxydopamine-induced Parkinson's disease in rats. Mol Neurobiol. https://doi.org/10.1007/s12035-018-1075-z
40. Sheline CT, Cai AL, Zhu J, Shi C (2010) Serum or target deprivation-induced neuronal death causes oxidative neuronal accumulation of Zn2+ and loss of NAD+. Eur J Neurosci 32:894–904
41. Medvedeva YV, Ji SG, Yin HZ, Weiss JH (2017) Differential vulnerability of CA1 versus CA3 pyramidal neurons after ischemia: possible relationship to sources of Zn2+ accumulation and its entry into and prolonged effects on mitochondria. J Neurosci 37:726–737
42. Chen Y, Irie Y, Keung WM, Maret W (2002) S-Nitrosothiols react preferentially with zinc thiolate clusters of metallothionein III through transnitrosation. Biochemistry 41:8360–8367
43. Abiria SA, Krapivinsky G, Sah R, Santa-Cruz AG, Chaudhuri D, Zhang J, Adstamongkonkul P, DeCaen PG et al (2017) TRPM7 senses oxidative stress to release Zn2+ from unique intracellular vesicles. Proc Natl Acad Sci U S A 114:E6079–E6088
44. Peng J, Peng L, Stevenson FF, Doctrow SR, Andersen JK (2007) Iron and paraquat as synergistic environmental risk factors in sporadic Parkinson's disease accelerate age-related neurodegeneration. J Neurosci 27:6914–6922
45. Peng J, Stevenson FF, Oo ML, Andersen JK (2009) Iron-enhanced paraquat-mediated dopaminergic cell death due to increased oxidative stress as a consequence of microglial activation. Free Radic Biol Med 46:312–320
46. Takeda A, Nakamura M, Fujii H, Uematsu C, Minamino T, Adlard PA, Bush AI, Tamano T (2014) Amyloid β-mediated Zn^{2+} influx into dentate granule cells transiently induces a short-term cognitive deficit. PLoS One 9:e115923